JACS
JOURNAL OF THE AMERICAN CHEMICAL SOCIETY
Communication
pubs.acs.org/JACS

Lanthanide-Loaded Erythrocytes As Highly Sensitive Chemical Exchange Saturation Transfer MRI Contrast Agents

Giuseppe Ferrauto,[†] Daniela Delli Castelli,[†] Enza Di Gregorio,[†] Sander Langereis,[‡] Dirk Burdinski,[‡] Holger Grüll,[‡] Enzo Terreno,[†] and Silvio Aime[†,*]

[†]Department of Molecular Biotechnology and Health Sciences, Molecular Imaging and Preclinical Centers, University of Torino, Torino, Italy

[‡]Department of Minimally Invasive Healthcare, Philips Research Europe, 5656 AE Eindhoven, The Netherlands

Supporting Information

ABSTRACT: Chemical exchange saturation transfer (CEST) agents are a new class of frequency-encoding MRI contrast agents with a great potential for molecular and cellular imaging. As for other established MRI contrast agents, the main drawback deals with their low sensitivity. The sensitivity issue may be tackled by increasing the number of exchanging protons involved in the transfer of saturated magnetization to the "bulk" water signal. Herein we show that the water molecules in the cytoplasm of red blood cells can be exploited as source of exchangeable protons provided that their chemical shift is properly shifted by the intracellular entrapment of a paramagnetic shift reagent. The sensitivity of this system is the highest displayed so far among CEST agents (less than 1 pM of cells), and the natural origin of this system makes it suitable for in vivo applications. The proposed Ln-loaded RBCs may be proposed as reporters of the blood volume in the tumor region.

Chemical exchange saturation transfer (CEST) agents[1−4] are a unique class of MRI contrast agents (CAs) that are currently under intense scrutiny for MR molecular imaging and MR image-guided drug delivery applications[5,6] The peculiarity of CEST agents is the frequency-encoding mechanism of contrast generation that can be switched *on* at will by irradiating, with a selective radio frequency (RF) field, the exchangeable water protons of the agent. In the field of cellular and molecular MR imaging, one of the main advantages of CEST agents relies on the possibility of detecting more than one agent in the same MR image.[7−9] The sensitivity of CEST agents can be dramatically increased by exploiting the huge number of exchangeable water protons entrapped in the cavity of nanovesicles such as liposomes (lipoCEST) or polymersomes.[10] In order to remove the isochronicity of the protons in the intra- and extravesicular compartments, a shift reagent (SR) is selectively entrapped in the inner aqueous cavity of the carrier. The performance of lipoCEST agents can be further improved by changing the shape of the liposomes. It has been demonstrated that the passage from spherical to nonspherical vesicles induces a large effect on the chemical shift of the water protons in the inner liposomal cavity.[11,12] In fact, the water resonance in the presence of a paramagnetic SR undergoes a shift that is due to the sum of the dipolar and the bulk magnetic susceptibility (BMS) effects. The former contribution requires a chemical interaction between the paramagnetic complexes and the water molecules, while the latter depends on the shape of the carrier in which the SR is confined. The analogy between liposomes and cells inspired us to explore the possibility of using cells as SR carriers in order to pursue their visualization by CEST contrast. Furthermore, a significant BMS effect can be also expected for cells as they are intrinsically more or less nonspherical objects and are known to orient themselves in magnetic fields.[13−16] The force that drives the orientation is the magnetic susceptibility anisotropy of the cellular membrane. In principle, any non-spherical cell type should be able to orient in a magnetic field, but in this work we chose human erythrocytes (red blood cells, RBCs) by virtue of their highly asymmetrical lenticular shape. RBCs were loaded with paramagnetic LnHPDO3A complexes (where Ln = Eu, Gd, Dy, Tm and Yb; Scheme 1) acting as shift reagents. Previous work established that these complexes are well tolerated by cells even at high intracellular concentrations.[17] Loading RBCs with LnHPDO3A chelates was performed using the hypotonic swelling procedure.[18] Briefly, RBCs were subjected to an osmotic gradient that induced swelling. (If the swelling is carried out in the presence of the complexes, the SRs can cross the cell membrane and accumulate in the cytosol.) The RBC morphology then was restored by returning the extracellular

Scheme 1. Ln-Loaded RBCs as CEST MRI CAs[a]

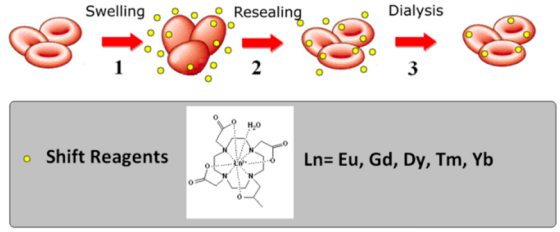

[a]RBCs are placed in hypotonic solution in the presence of LnHPDO3A, allowing internalization of the SR (step 1). Next, the external medium is brought to an isotonic osmolarity, and the morphology of the cells is restored (i.e. resealing of the RBCs, step 2). Step 3, the Ln-loaded cells are washed with PBS to eliminate the SR molecules that have not been internalized.

Received: November 25, 2013
Published: December 23, 2013

dx.doi.org/10.1021/ja411793u | J. Am. Chem. Soc. 2014, 136, 638−641

environment to the original isotonic conditions (Scheme 1). All the main hematological parameters (number of RBCs, MCV, MCH, and MCHC) were preserved upon this treatment (Table S1 in the Supporting Information [SI]). The average intracellular concentration of LnHPDO3A in the RBCs was in the range 4.5−4.8 mM as determined by ICP-MS (see Table S2 in SI).

The CEST properties of the Ln-loaded RBCs (compared to nonloaded RBCs) were assessed at 7.1 T. A saturation scheme consisting of a continuous rectangular wave pulse of 2 s with a RF intensity of 3 μT was used. The Z-spectrum and the corresponding ST% profile obtained for DyHPDO3A-loaded RBCs (*black*) and control cells (*red*) are reported in Figure 1.

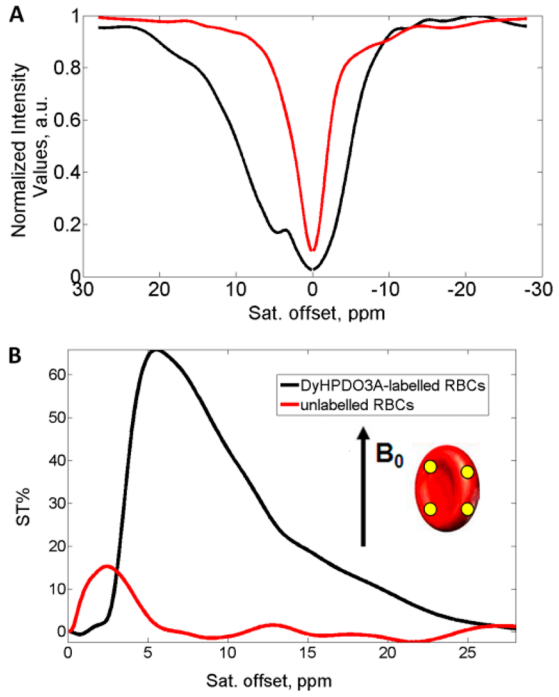

Figure 1. Z-spectrum (A) and ST profile (B) of DyHPDO3A-loaded RBCs (*black*) and control RBCs (*red*).

The right-hand asymmetry of the Z-spectrum and the corresponding CEST effect observed at 2−3 ppm downfield of the water resonance peak for the native RBCs is caused by the pool of exchanging protons, from species naturally present in erythrocytes.[19] Although the observed chemical shift might be affected by the discoidal shape of RBCs and by the content of paramagnetic deoxyhemoglobin, the CEST peak seems to be dominated by the exchange of −OH groups in monomeric and polymeric sugars. When RBCs were loaded with DyHPDO3A, the Z-spectrum and the CEST effect was markedly different from the native erythrocytes. The SR-loaded cells displayed an evident asymmetry centered at 6.5 ppm (Figure 1A) with a corresponding ST% value of 65% (Figure 1B). The increase of the bandwidth is due to the overall decrease of T_2* as a consequence of the paramagnetic loading. In principle, the observed shift of 6.5 ppm is the sum of the dipolar and BMS contributions. However, the dipolar term can be estimated from the amount of shift reagent internalized in RBCs (4.5 mM, see Table S2 in SI) and the molar shift reported for DyHPDO3A (∼−19 ppm/M).[21] The computed value (−0.085 ppm) represents less than 2% of the observed shift, thereby indicating that the shift of the intracellular water protons is almost fully ascribable to the BMS contribution. In close analogy to what was previously found for lipoCEST agents, the BMS-induced chemical shift of the intracellular water resonance can be modulated by changing the effective magnetic moment (μ_{eff}) of the lanthanide ion or the amount of SR internalized in RBCs,[20,22] through the following relationship: BMS $\propto \mu_{eff}^2 \times [Ln^{3+}]$

The imaging characteristics (T_{2w} map, T_{1w} map, Z- and CEST-spectra) of RBCs labeled with different LnHPDO3A complexes are shown in Figure 2. As the intracellular concentrations of the

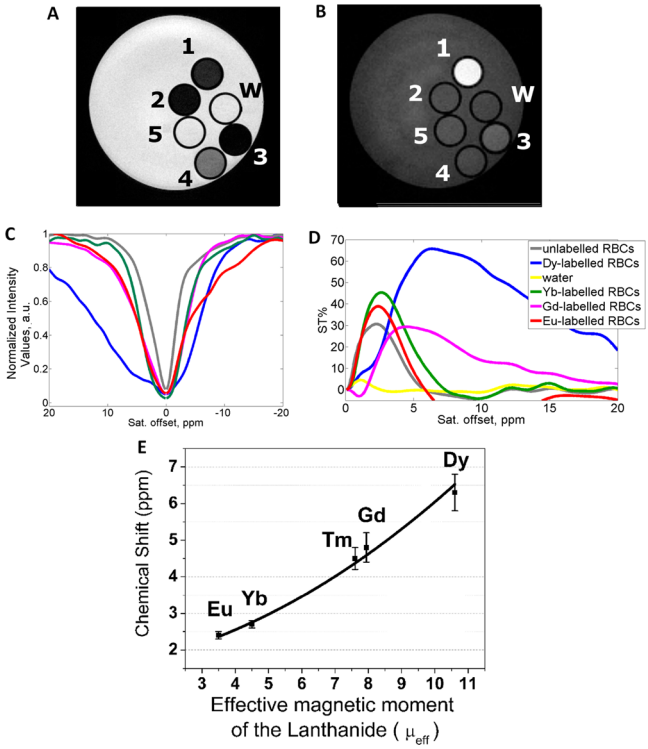

Figure 2. (A) T_{2w} and (B) T_{1w} maps of a phantom consisting of glass capillaries containing RBCs loaded with (1) GdHPDO3A, (2) EuHPDO3A, (3) DyHPDO3A, (4) YbHPDO3A, (5) unloaded RBCs. (C) Z-spectra and (D) ST values of the RBC samples. (E) Relationship between μ_{eff} of the lanthanide and the chemical shift of CEST absorption. The line in E has been added to aid the visualization of the trend.

different LnHPDO3A complexes within the RBCs (i.e. the $[Ln^{3+}]$ term) are comparable (see Table S2), the differences in the chemical shift values can be attributed to the μ_{eff} values of the metal ions (μ_{eff} = 3.5 for Eu, 7.94 for Gd, 10.6 for Dy, 7.6 for Tm, and 4.5 for Yb). The data plotted in Figure 2E support this hypothesis. Moreover, such data also provide a further confirmation of the predominance of the BMS effect. In fact, the dipolar contribution should be null for Gd-based complexes,[10b] and the sign of the shift should be dependent on the magnetic anisotropy of the Ln(III) ion (positive for Eu, Tm, and Yb and negative for Dy). The experimental data reported in Figure 2E do not match both these expectations.

A change in sign of the BMS shift can be pursued by the incorporation of lipid-functionalized lanthanide complexes in the membrane (Figure 3A). The rationale is that the sign of the BMS shift is dependent on the orientation of cells within the magnetic field. Such an orientation arises from the interaction of the external magnetic field and the magnetic anisotropy of the cell membrane ($\Delta\chi$). Thus, the orientation in the field can be flipped by 90° upon incorporating in the membrane a paramagnetic

dx.doi.org/10.1021/ja411793u | J. Am. Chem. Soc. 2014, 136, 638−641

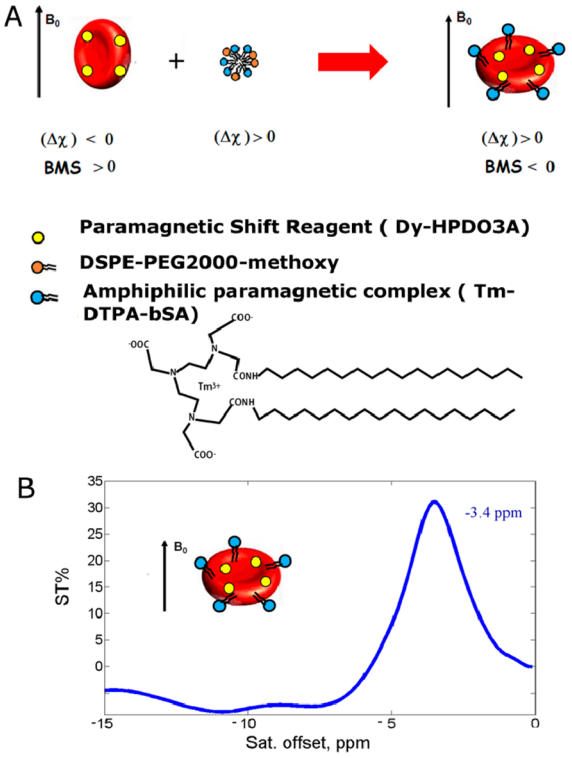

Figure 3. (A) Scheme of the interaction between RBCs and Tm-containing micelles. (B) ST-spectrum of DyHPDO3A-loaded RBCs after incorporation of Tm in the cellular membrane. The decrease of Dy-concentration (from 4.5 to 2.8 mM) might be ascribed to a transient leakage of the erythrocyte membrane upon the interaction with the Tm-micelles.

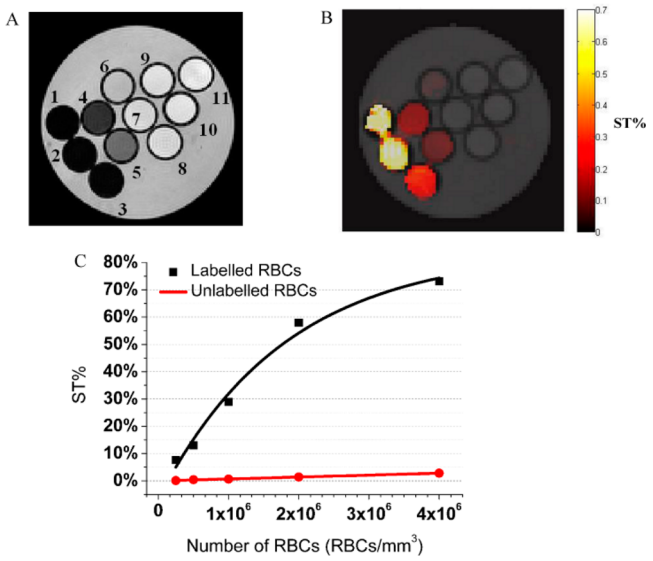

Figure 4. (A) T_2-weighted image (T_{2w}) and (B) saturation transfer map (STmap) calculated at 5.6 ppm, of a phantom containing Dy-labeled (1−5) or unlabeled (6−10) RBCs in a concentration range of 1×10^6 to 4×10^6/ mm^3. Capillary 11 contains PBS. The exact composition of the 10 tubes is reported in the caption of Figure S1 in SI. (C) Correlation between number of RBCs/mm^3 and ST% for labeled (*black*) and unlabeled (*red*) cells. The lines added in C have been added to aid the visualization of the trend.

complex with a magnetic anisotropy of opposite sign with respect to the "natural" anisotropy of the carrier ($\Delta\chi < 0$ in case of phospholipid-based systems, Figure 3A).[21] It has been reported that the Tm-DTPA-bSA complex (Figure 3A) is able to change the orientation of bicelles or lipoCEST from parallel to perpendicular to the field.[12] To check if the same phenomenon applies to Ln-loaded RBCs, the cellular membrane of DyHPDO3A-loaded RBCs was labeled with Tm-DTPA-bSA by incubating cells in the presence of micelles composed by Tm-DTPA-bSA (60 mol %) and DSPE-PEG2000 (40 mol %) (Figure 3A). Incorporation of the Tm-based compound in the RBC membrane occurred via lipid exchange similar to that reported for liposomes.[23] After the incubation with the paramagnetic micelles, RBCs were extensively washed. As shown in Figure 3B, the Z-spectrum of the Tm-labeled, Dy-loaded RBCs displayed a ST effect of ∼30% at a negative shift offset (−3.4 ppm from the bulk water signal), as expected on the basis of the change in the orientation of the cells in the field. The observed chemical shift is in line with the amount of internalized DyHPDO3A (∼2.7 mM) as measured by ICP-MS (Table S3).

To estimate the sensitivity of the herein reported cellular CEST agents, the detection limit of DyHPDO3A-loaded RBCs was assessed by successive dilutions in phosphate buffered saline (PBS). Figure 4 shows the CEST effect decreased with dilutions, but it was still detectable up to $\sim 2.5 \times 10^5$ cells/mm^3 (corresponding to ∼5% of physiologically circulating RBCs). This result is very promising in view of potential in vivo detection of RBCs using CEST MR imaging. Figure 4C shows the unlabeled RBCs did not have a significant effect (ST% < 5%) at the specific frequency of the intracellular shifted water nor at the higher number of cells used. Z- and CEST-spectra of all specimens are reported in Figure S1 in SI. It is worth noting that the required RF saturation intensity (3 μT) is similar to the values used in clinical applications.[24]

In a related experiment, the Dy-loaded RBCs were diluted into unlabeled RBCs, and the detection threshold was the same as that measured upon diluting the RBCs in buffer (Figure S2 in SI). As proof of principle of the possibility to apply Ln-loaded RBCs in vivo, maps of vascular distribution upon injection of Dy-loaded RBCs have been acquired. Dy-RBCs have been prepared as described above and injected into the mouse tail vein, in mice bearing xenograft tumors (Figure 5A, T_{2w} image of the tumor).

The absorption frequency of the used Dy-loaded RBCs, as evaluated by acquiring Z- and ST spectra in the NMR tube containing the labeled RBCs in PBS centered at 4 ppm (Figure 5B). The Z-spectrum of the tumor region shows the visualization of a specific ST% of ∼5% at 4 ppm from water, a ST effect not present before the administration of Dy-loaded RBCs (Figure 5C). The STmap obtained with the RF field offset at 4 ppm (Figure 5D) shows that the ST% is not homogeneous in the tumor region, which indicates the heterogeneity of the blood vessel distribution in the tumor mass.

In conclusion, Ln-loaded RBCs represent an innovative and highly sensitive new entry in the family of CEST MRI contrast agents. This system has been herein named ErythroCEST. The occurrence of a positive intracellular water shift upon using Dy- or GdHPDO3A-loaded RBCs corroborates the view that erythrocytes are able to orient themselves into a magnetic field. The ability to switch the sign of BMS after the interaction with the paramagnetic micelles is definitively ascribable to the change in the orientation of erythrocytes in the magnetic field. The unprecedented reported sensitivity of this system (<1 pM in terms of cell concentration, corresponding to ∼2 mM of DyHPDO3A), the use of an endogenous system, and the safe saturation scheme make this kind of contrast agent very

dx.doi.org/10.1021/ja411793u | J. Am. Chem. Soc. 2014, 136, 638−641

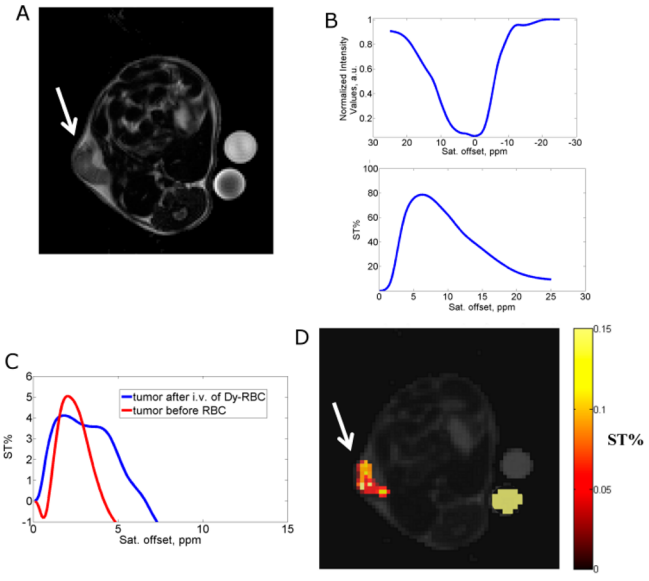

Figure 5. (A) T_2-weighted image (T_{2w}) of a mouse bearing a subcutaneous tumor (white arrow). (B) Z- and ST- spectra of Dy-loaded RBCs in the reference tube. (C) ST-spectra of tumor region pre- and post-Dy-RBCs injection. (D) ST map at 4 ppm for vascular volume map.

promising for future clinical applications. In particular, since this system is fully retained inside the vascular system, it may be useful for assessing the vascular volume in the presence of other CEST agents designed to report about other hallmarks of a given pathology. The presence of LnHPDO3A-labeled RBCs in the blood circuit do not yield any detectable adverse effect on the mice's health. However, a contrast enhancement was detected in the spleen for ~3 weeks, as expected, this being an organ committed to physiologically processing "old" erythrocytes

■ ASSOCIATED CONTENT

Ⓢ Supporting Information

Experimental procedures. This material is available free of charge via the Internet at http://pubs.acs.org.

■ AUTHOR INFORMATION

Corresponding Author

silvio.aime@unito.it

Notes

The authors declare no competing financial interest.

■ ACKNOWLEDGMENTS

This work was supported by funding from local government (Regione Piemonte, PIIMDMT and Nano-IGT projects), MIUR (PRIN 2009), and EU-FP7 integrated project ENCITE. Scientific support from Bracco Imaging SpA and CIRCMSB (Consorzio Interuniversitario di Ricerca sulla Chimica dei Metalli nei Sistemi Biologici) is also gratefully acknowledged.

■ REFERENCES

(1) Ward, K. M.; Aletras, A. H.; Balaban, R. S. *J. Magn. Reson.* **2000**, *143*, 79.

(2) Sherry, A. D.; Woods, M. *Annu. Rev. Biomed. Eng.* **2008**, *10*, 391.

(3) Terreno, E.; Delli Castelli, D.; Aime, S. *CMMI* **2010**, *5*, 78.

(4) Zhang, S.; Merritt, M.; Woessner, D. E.; Lenkinski, R. E.; Sherry, D. *Acc. Chem. Res.* **2003**, *36*, 783.

(5) Langereis, S.; Keupp, J.; van Velthoven, J. L.; de Roos, I. H.; Burdinski, D.; Pikkemaat, J. A.; Grüll, H. *J. Am. Chem. Soc.* **2009**, *131*, 1380.

(6) Burdinski, D.; Pikkemaat, J. A.; Emrullahoglu, M.; Costantini, F.; Verboom, W.; Langereis, S.; Grüll, H.; Huskens, J. *Angew. Chem., Int. Ed.* **2010**, *49*, 2227.

(7) (a) Ferrauto, G.; Delli Castelli, D.; Terreno, E.; Aime, S. *Magn. Reson. Med.* **2013**, *69*, 1703−11. (b) Gianolio, E.; Stefanìa, R.; Di Gregorio, E.; Aime, S. *Eur. J. Inorg. Chem.* **2012**, 1934.

(8) Aime, S.; Carrera, C.; Delli Castelli, D.; Geninatti Crich, S.; Terreno, E. *Angew.Chem. Int. Ed.* **2005**, *44*, 1813.

(9) McMahon, M. T.; Gilad, A. A.; DeLiso, M. A.; Cromer Berman, S. M.; Bulte, J. W. M.; van Zijl, P. C. M. *Magn. Reson. Med.* **2008**, *60*, 803.

(10) (a) Aime, S.; Delli Castelli, D.; Terreno, E. *Angew. Chem., Int. Ed.* **2005**, *44*, 5513. (b) Terreno, E.; Cabella, C.; Carrera, C.; Delli Castelli, D.; Mazzon, R.; Rollet, S.; Stancanello, J.; Visigalli, M.; Aime, S. *Angew. Chem., Int. Ed.* **2007**, *46*, 966. (c) Grüll, H.; Langereis, S.; Messager, L.; Delli Castelli, D.; Sanino, A.; Torres, E.; Terreno, E.; Aime, S. *Soft Matter* **2010**, *6*, 4847.

(11) Terreno, E.; Delli Castelli, D.; Violante, E.; Sanders, H. M.; Sommerdijk, N. A.; Aime, S. *Chemistry* **2009**, *15*, 1440.

(12) Aime, S.; Delli Castelli, D.; Terreno, E. *Methods Enzymol.* **2009**, *464*, 193−210.

(13) Murayama, M. *Nature* **1965**, *206*, 420−422.

(14) Miyakoshi, J. *Prog. Biophys. Mol. Biol.* **2005**, *87*, 231−223.

(15) Higashi, T.; Yamagishi, A.; Takeuchi, T.; Sagawa, S.; Onishi, S.; Date, M. *Blood* **1993**, *82*, 1328−1334.

(16) Higashi, T.; Sagawa, S.; Ashida, N.; Takeuchi, N. *Bioelectromagnetics* **1996**, *17*, 335.

(17) Di Gregorio, E.; Gianolio, E.; Stefânia, R.; Barutello, G.; Digilio, G.; Aime, S. *Anal. Chem.* **2013**, *85*, 5627.

(18) (a) Rossi, L.; Serafini, S.; Pierigé, F.; Cerasi, A. A.; Fraternale, A.; Chiarantini, L.; Magnani, M. *Expert. Opin. Drug Delivery* **2005**, *2*, 311. (b) Antonelli, A.; Sfara, C.; Manuali, E.; Bruce, I. J.; Magnani, M. *Nanomedicine (London)* **2011**, *6*, 211. (c) Johnson, K. M.; Zang Tao, J.; Kennan, R. P.; Gore, J. C. *Magn. Reson. Med.* **1998**, *40*, 133. (d) Millan, C. G.; Sayalero Marinero, M. L.; Castaneda, A. Z.; Lanao, J. M. *J. Controlled Release* **2004**, *95*, 27. (e) Hamidi, M.; Zarrin, A. H.; Foroozesh, M.; Zarei, N.; Mohammadi-Samani, S. *Int. J. Pharm.* **2007**, *341*, 125. (f) Johnson, K. M.; Tao, J. Z.; Kennan, R. P.; Gore, J. C. *Magn. Reson. Med.* **1998**, *40*, 133.

(19) van Zijl, P. C. M.; Yadav, N. N. *Magn. Reson. Med.* **2011**, *65*, 927.

(20) Peters, J. A.; Huskens, J.; Raber, D. J. *Prog. Nucl. Magn. Reson. Spectrosc.* **1996**, *28*, 283.

(21) Aime, S.; Geninatti Crich, S.; Gianolio, E.; Giovenzana, G. B.; Tei, L.; Terreno, E. *Coord. Chem. Rev.* **2006**, *250*, 1562.

(22) (a) Aime, S.; Delli Castelli, D.; Terreno, E. *Methods Enzymol.* **2009**, *464*, 193. (b) Terreno, E.; Barge, A.; Beltrami, L.; Cravotto, G.; Dell Castelli, D.; Fedeli, F.; Jebasingh, B.; Aime, S. *Chem. Commun. (Cambridge)* **2008**, *5*, 600.

(23) (a) Ishida, T.; Iden, D. L.; Allen, T. M. *FEBS Lett.* **1999**, *460*, 129−133. (b) Takasaki, J.; Ansell, S. M. *Bioconjugate Chem.* **2006**, *17*, 438.

(24) Yadav, N. N.; Jones, C. K.; Hua, J.; Xu, J.; van Zijl, M. P. C. *Magn. Reson. Med.* **2013**, *69*, 966.